Preparation and characterization for multicomponent crystals of the antidiabetic drug gliquidone based on crystal engineering

Lina Jia[†], Yang Yu[†], Mengwei Wang[†], Hanzhi Ouyang[†] and Junbo Gong[*, †, ‡, §]

[†] State Key Laboratory of Chemical Engineering, School of Chemical Engineering and Technology, Tianjin University, Tianjin 300072, P. R. China

[‡] Collaborative Innovation Center of Chemistry Science and Engineering, Tianjin 300072, P. R. China

[§] Key Laboratory Modern Drug Delivery and High Efficiency in Tianjin University, Tianjin 300072, P. R. China

Contents of Supporting Information

Figure S1

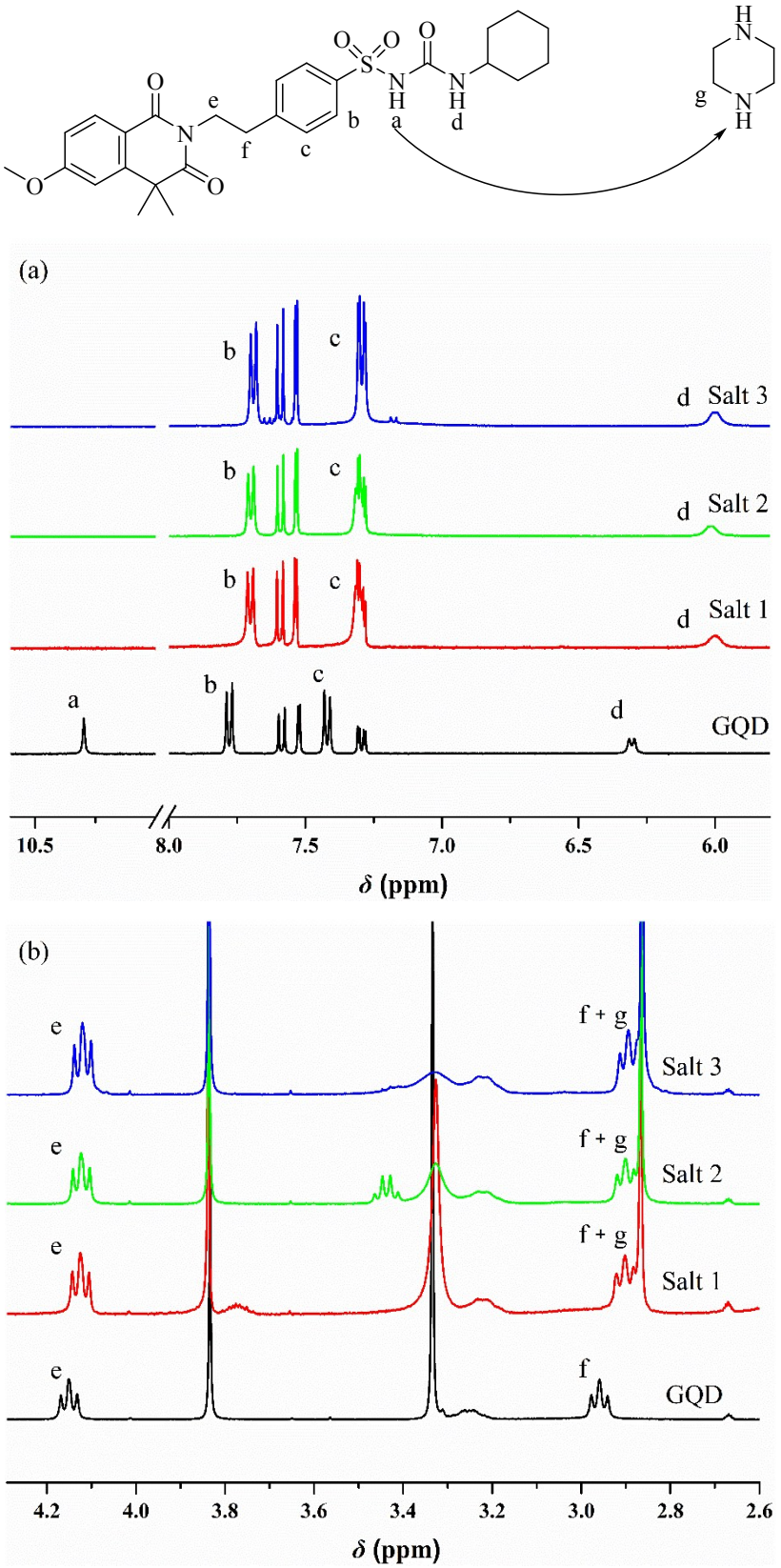
(a)
b
c
d
Salt 3
Salt 2
Salt 1
a
GQD
10.5
8.0
7.5
7.0
6.5
6.0
δ (ppm)
(b)
e
f + g
f
4.2
4.0
3.8
3.6
3.4
3.2
3.0
2.8
2.6
δ (ppm)

Figure S1. ^{1}H NMR data recorded in DMSO-d_6 solution for GQD, salt 1, salt 2 and salt 3. The ^{1}H spectra were obtained using a Bruker Advance III NMR spectrometer operating at 400 MHz. The proton transfer from GQD can clearly be seen from δ_a, δ_b, δ_c, δ_d, δ_e and δ_f in (a), the ratio of GQD and PPZ can be seen from δ_f, 2.94 (t, 2H, J = 9 Hz) and δ_g, 2.89 (m, 6H) in (b).

Figure S2

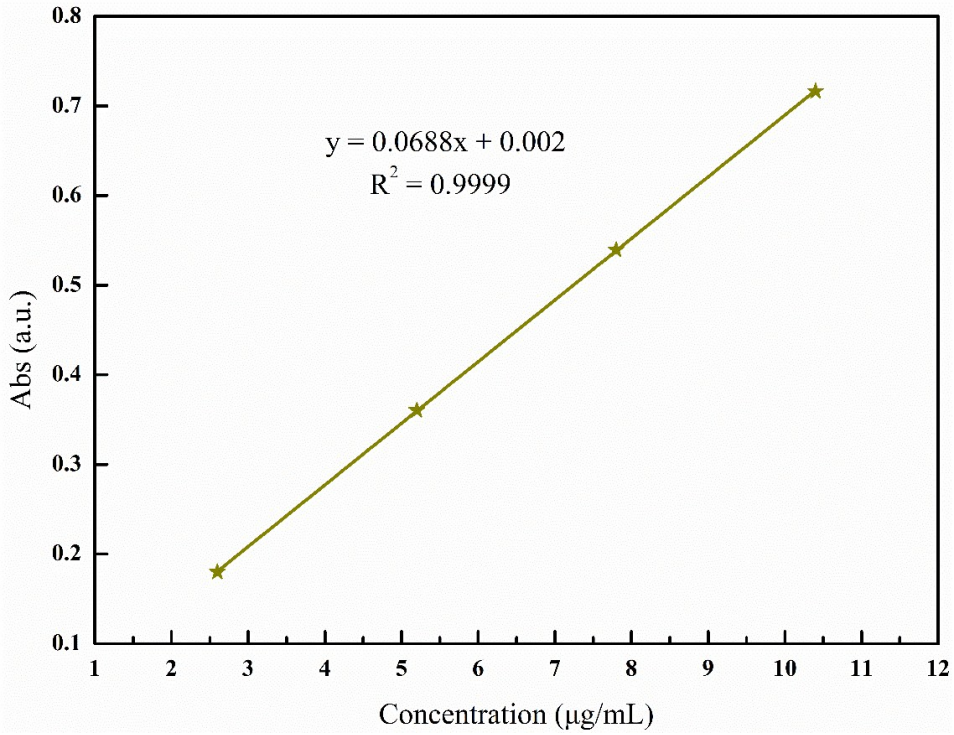

Figure S2. UV standard curve.

Scheme S1

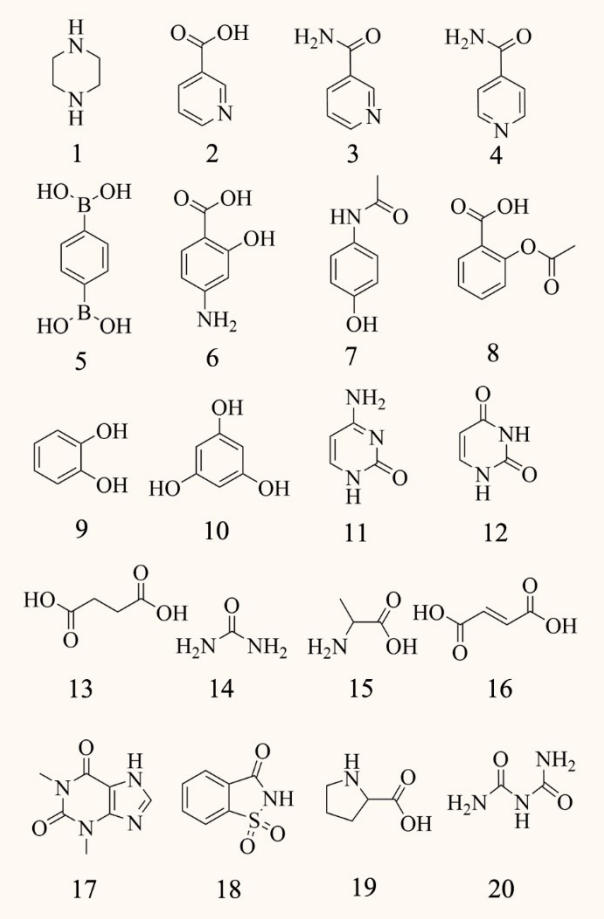

Scheme S1. The structures of selected co-formers.

Table S1

Table S1. The parameters of the selected co-formers.

Compound	Name	Formula	Donor	Acceptor	pKa 1	pKa 2
1	Piperazine	$C_4H_{10}N_2$	2	2	9.7	5.3
2	Nicotinic acid[b]	$C_6H_5NO_2$	1	3	4.9	2.0
3	Nicotinamide	$C_6H_6N_2O$	2	3	3.5	14.8
4	Isonicotinamide	$C_6H_6N_2O$	2	3	3.4	15.0
5	*p*-BenDibA [ab]	$C_6H_8B_2O_4$	4	4	8.3	
6	4-ASA	$C_7H_7NO_3$	4	4	2.1	13.2
7	Paracetamol	$C_8H_9NO_2$	2	3	1.7	9.9
8	ASA	$C_9H_8O_4$	1	4	3.5	
9	Catechol[b]	$C_6H_6O_2$	2	2	9.5	12.1
10	Phloroglucinol	$C_6H_6O_3$	3	3	8.0	9.2
11	Cytosine	$C_4H_5N_3O$	3	4	4.2	9.0
12	Uracil	$C_4H_4N_2O_2$	2	4	4.2	8.6
13	Succinic acid[b]	$C_4H_6O_4$	2	4	4.2	5.6
14	Urea	CH_4N_2O	4	3	0.1	
15	Alamine	$C_3H_7NO_2$	3	3	2.4	9.9
16	Maleic acid[b]	$C_4H_4O_4$	2	4	1.9	6.2
17	Theophylline[b]	$C_7H_8N_4O_2$	1	6	1.6	8.6
18	Saccharin	$C_7H_5O_3NS$	1	4	2.0	
19	Proline	$C_5H_9NO_2$	2	3	2.0	10.6
20	Biuret [a]	$C_2H_5N_3O_2$	5	5	10.2	

[a] is predicted pka from SciFinder;

[b] forms co-crystals with sulfonylureas;

p-BenDibA is 1,4-Phenylenebisboronic acid; 4-ASA is 4-Aminosalicylic acid; ASA is Amino salicylic acid.

Figure S3

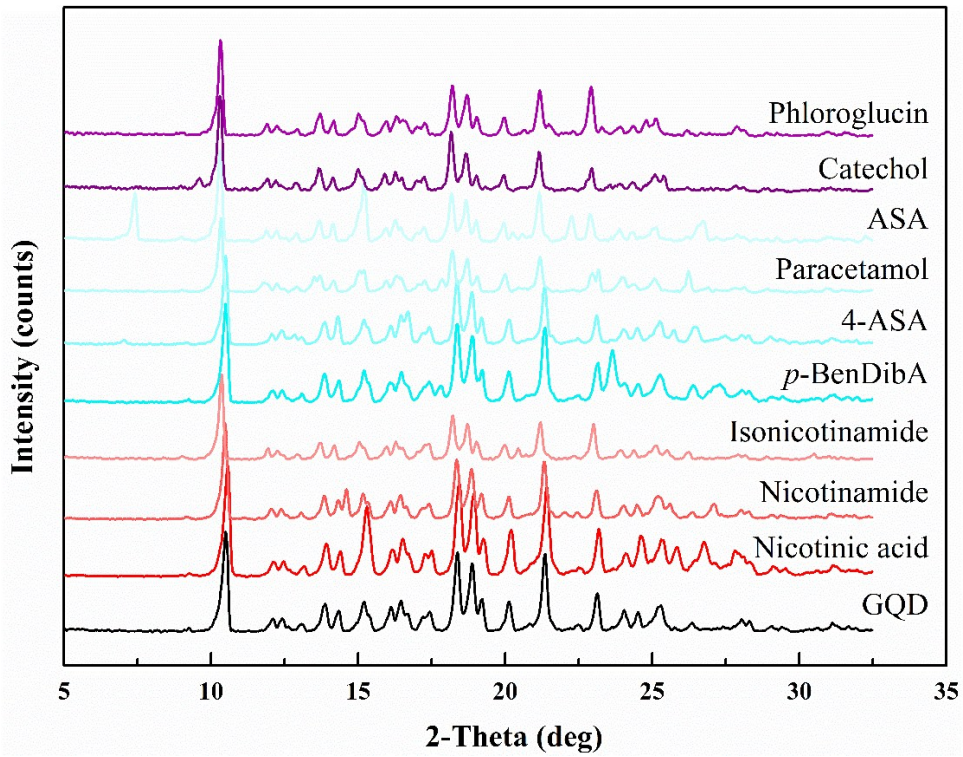

(b)

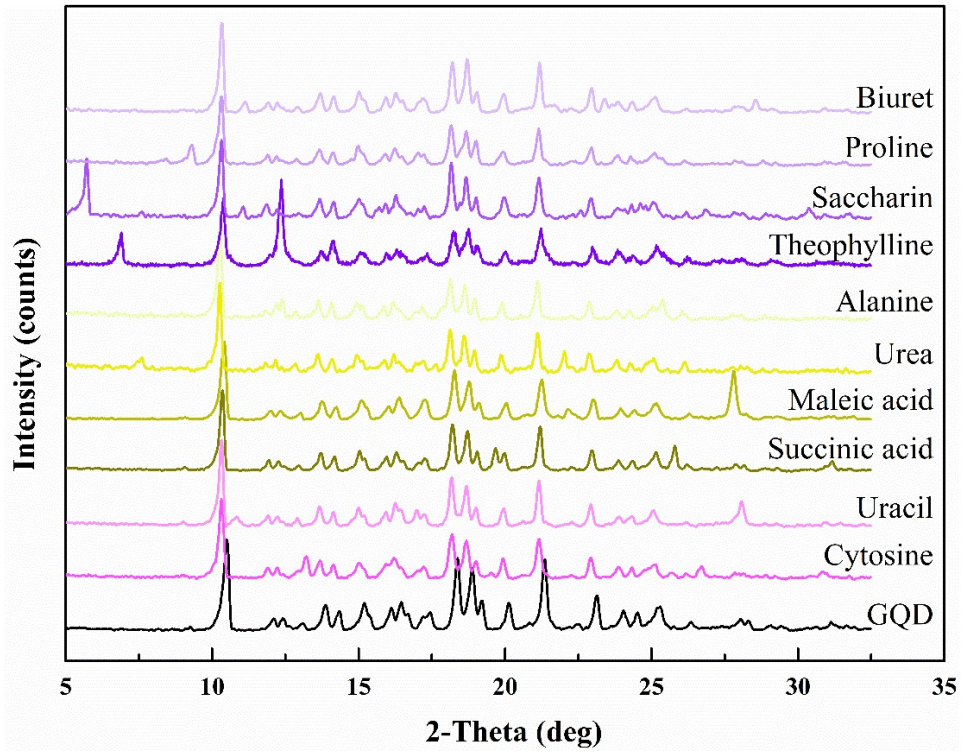

(b)

Figure S3. PXRD patterns of the eutectics (The PXRD of co-former is not shown for clarity).

Figure S4

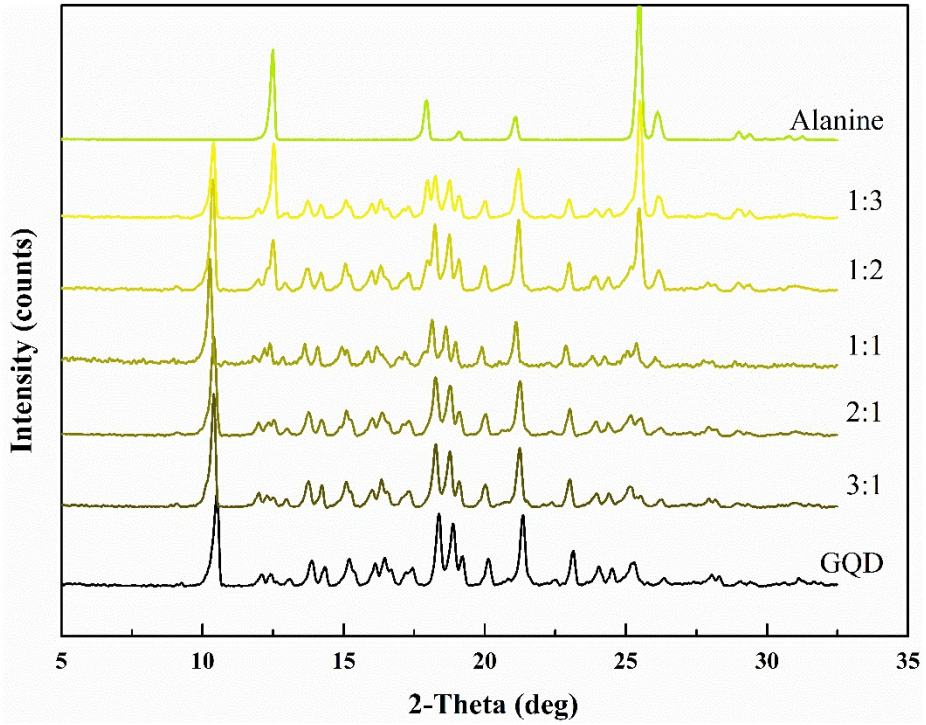

(a)

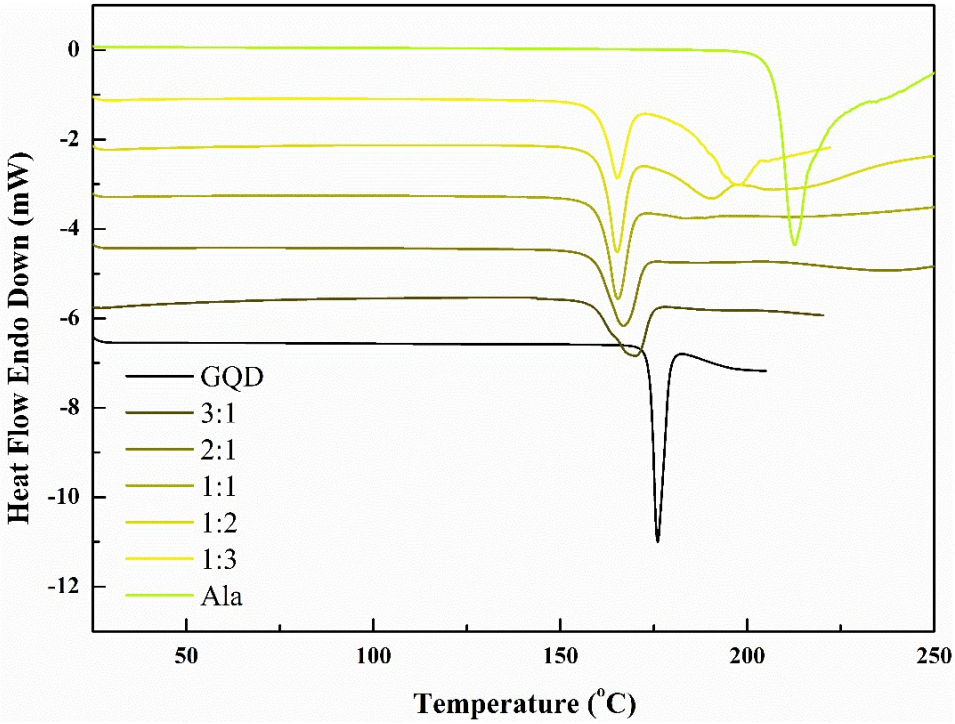

(b)

Figure S4. (a) PXRD patterns and (b) DSC profiles of the GQD-alanine eutectics with different ratios.

Figure S5

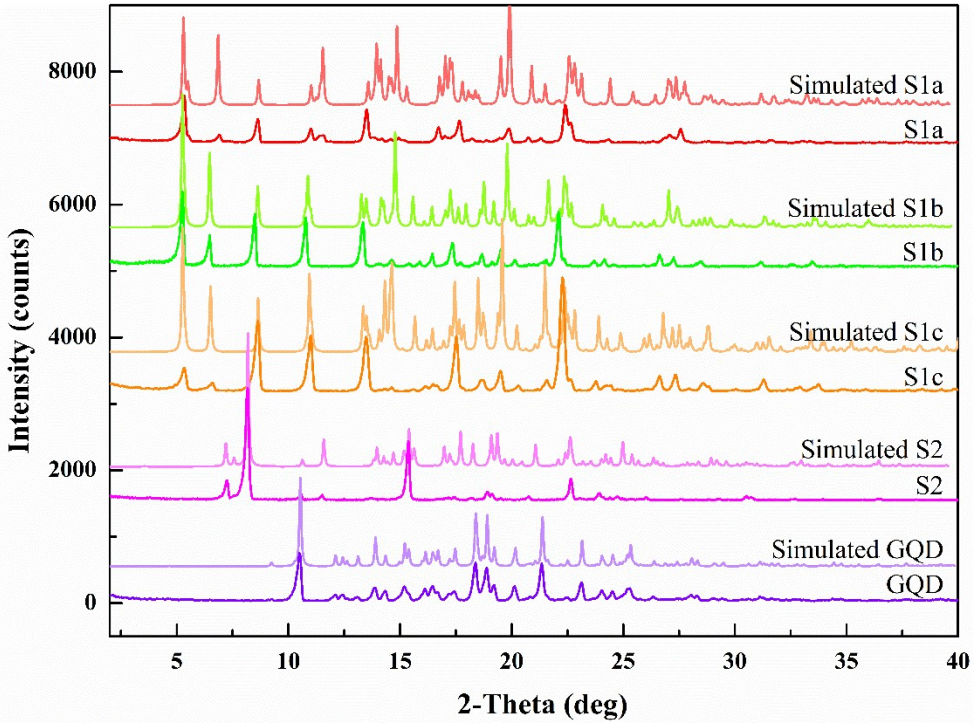

Figure S5. The comparations between PXRD generated from simulation and PXRD acquired from experiments.

Table S2

Table S2. Hydrogen bonds of GQD and its salts.

GQD	D–H···A	d (D–H) (Å)	d (H···A) (Å)	d (D···A) (Å)	θ (DHA) (°)
	N_2-H···O_2	0.86	2.06	2.880(2)	158.8
	N_3-H···O_5	0.86	2.14	2.832(2)	137.5
	N_3-H···O_5	0.86	2.53	3.246(2)	141.6
Salt S1a	D–H···A	d (D–H) (Å)	d (H···A) (Å)	d (D···A) (Å)	θ (DHA) (°)
	C_{1P}–H···O_5	0.99	2.38	3.155(2)	134.8
	N_{1P}–H···O_6	0.91(2)	1.99(2)	2.760(2)	142.3(19)
	N_3–H···O_{1S}	0.90(2)	2.02(2)	2.888(2)	161(2)
	O_{1S}–H···O_6	0.84	1.84	2.678(2)	171.1
	N_{1P}–H···N_2	1.011(19)	1.747(19)	2.749(2)	170.8(18)
Salt S1b	D–H···A	d (D–H) (Å)	d (H···A) (Å)	d (D···A) (Å)	θ (DHA) (°)
	C_{2P}–H···O_5	0.99	2.42	3.164(4)	131.7
	N_{1P}–H···O_5	0.97(3)	2.15(3)	2.953(3)	140(2)
	N_{1P}–H···O_6	0.97(3)	2.06(3)	2.804(4)	133(2)

	N_3–H···O_{1S}	0.83(3)	2.14(3)	2.955(4)	170(4)
	O_{1S}–H···O_6	0.84	1.89	2.726(3)	171.2
	N_{1P}–H···N_2	0.95(4)	1.84(4)	2.778(4)	167(3)
Salt S1c	D–H···A	d (D–H) (Å)	d (H···A) (Å)	d (D···A) (Å)	θ (DHA) (°)
	C_{2P}–H···O_5	0.99	2.40	3.165(5)	133.2
	N_{1P}–H···O_5	0.98(4)	2.14(4)	2.972(5)	142(3)
	N_{1P}–H···O_6	0.98(4)	2.04(4)	2.798(5)	132(3)
	N_3–H···O_{1S}	0.87(5)	2.04(5)	2.892(5)	166(5)
	O_{1S}–H···O_6	0.84	1.87	2.687(4)	165.5
	N_{1P}–H···N_2	0.99(7)	1.83(7)	2.780(5)	161(5)
Salt S2	D–H···A	d (D–H) (Å)	d (H···A) (Å)	d (D···A) (Å)	θ (DHA) (°)
	C_1–H···O_3	0.93	2.57	3.446(3)	157.1
	N_{1P}–H···O_5	0.91(3)	2.24(3)	2.910(2)	131(2)
	N_{1P}–H···O_6	0.91(3)	1.97(3)	2.744(2)	142(2)
	N_3–H···O_{1S}	0.86	2.13	2.934(3)	154.7
	O_{1S}–H···O_6	0.82	1.91	2.717(2)	168.4
	N_{1P}–H···N_2	0.80(3)	2.04(3)	2.829(2)	169(2)

Figure S6

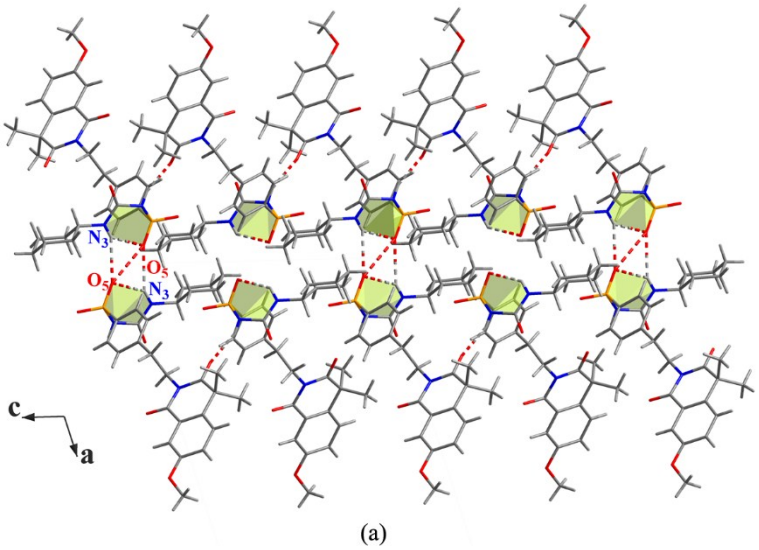

(a)

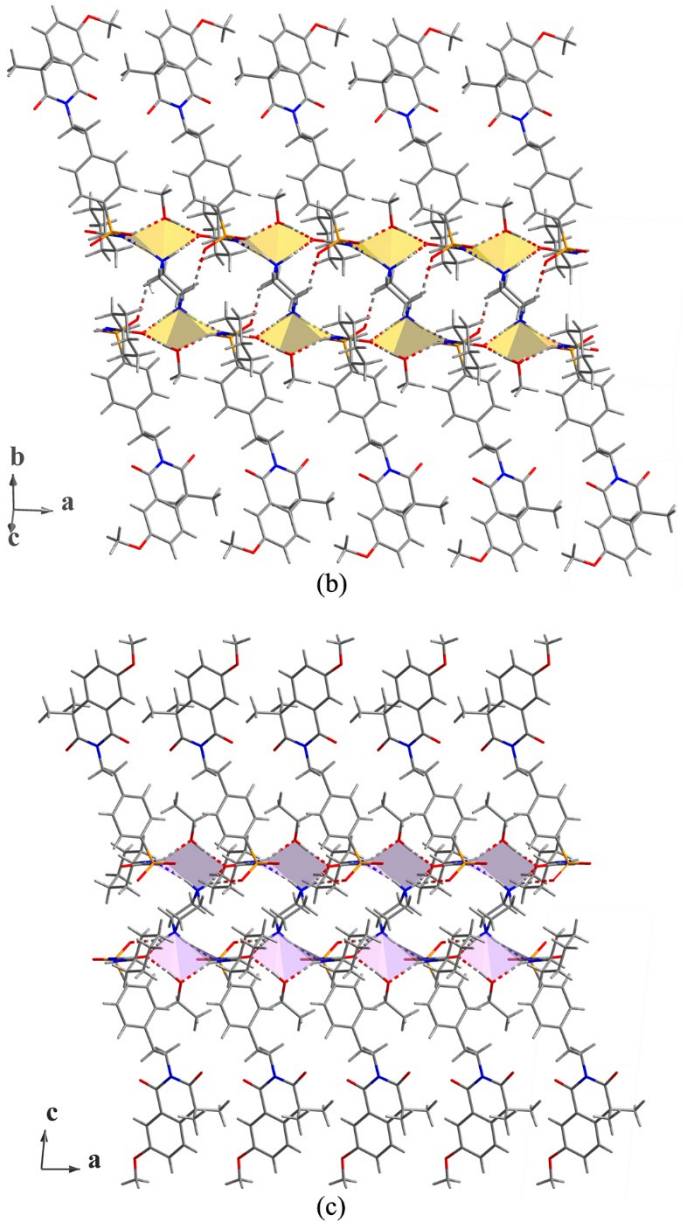

Figure S6. 2D H-bonding packing of various forms, (a) GQD, (b) salt S1a and (c) salt S2.

Figure S7

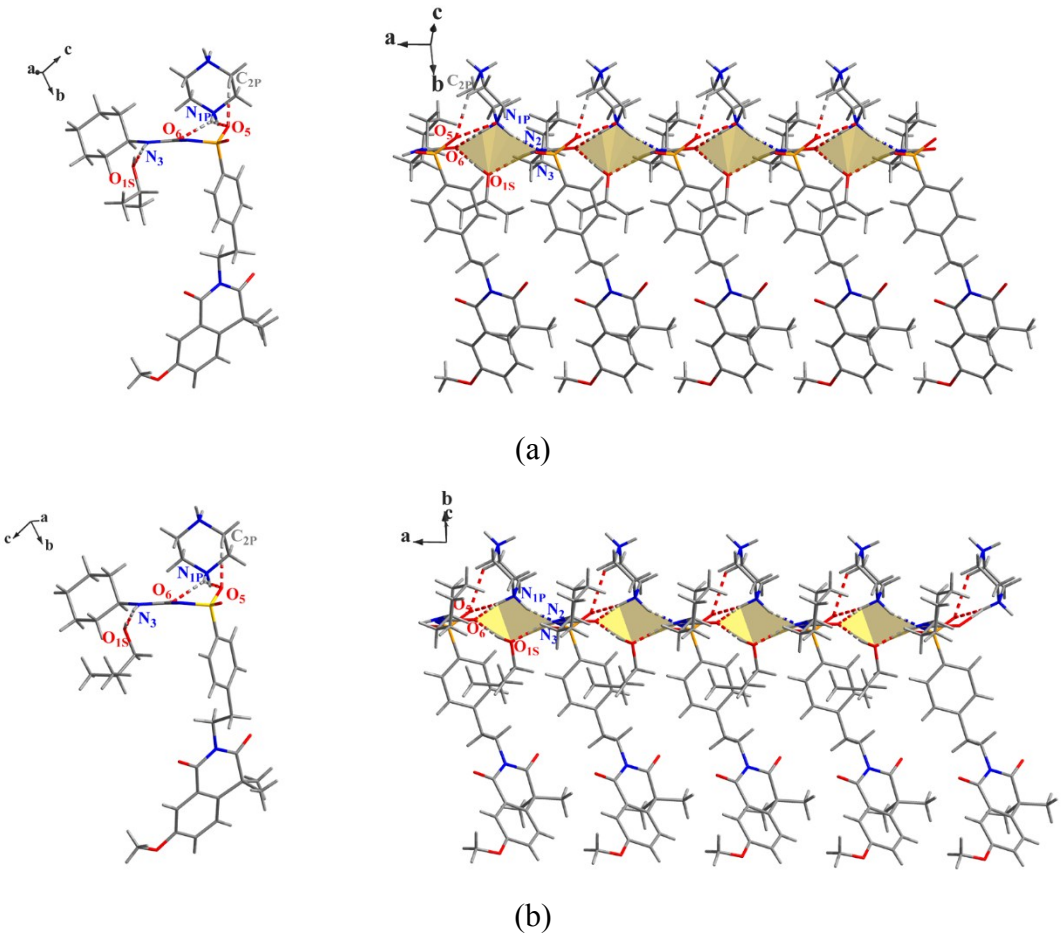

Figure S7. 1D chain in salts S1b (a) and S1c (b).

Figure S8

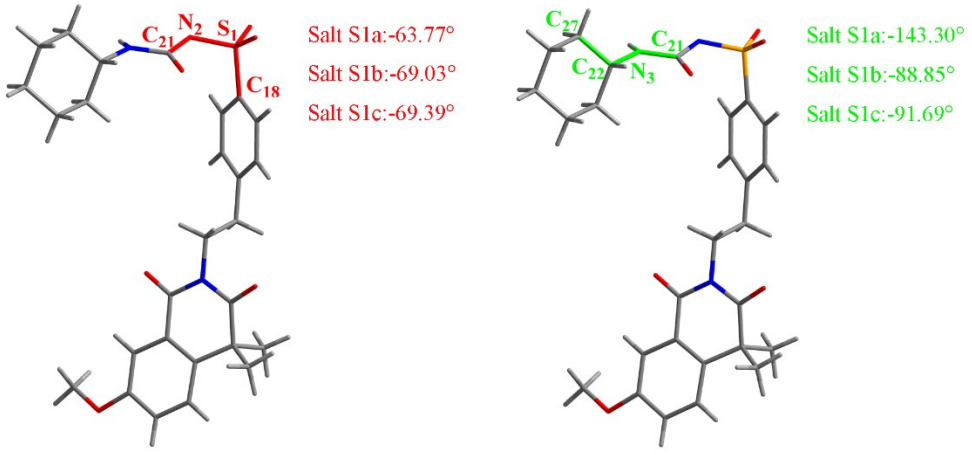

Figure S8. Comparisons of torsion angles between salts S1a, S1b and S1c.

Figure S9

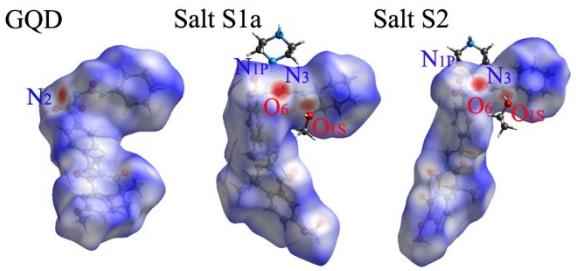

Figure S9. Hirshfeld surface generated on d_{norm} parameters.

Figure S10

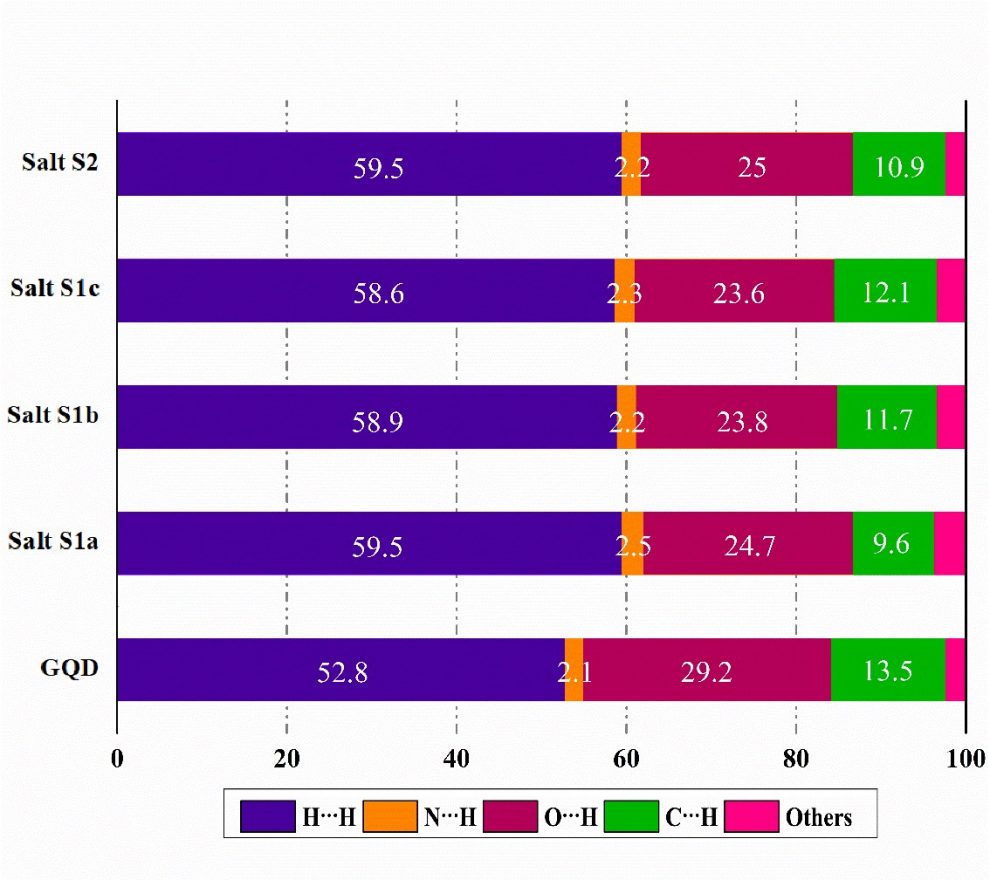

Figure S10. Percentage contributions to the Hirshfeld surface area.

Figure S11

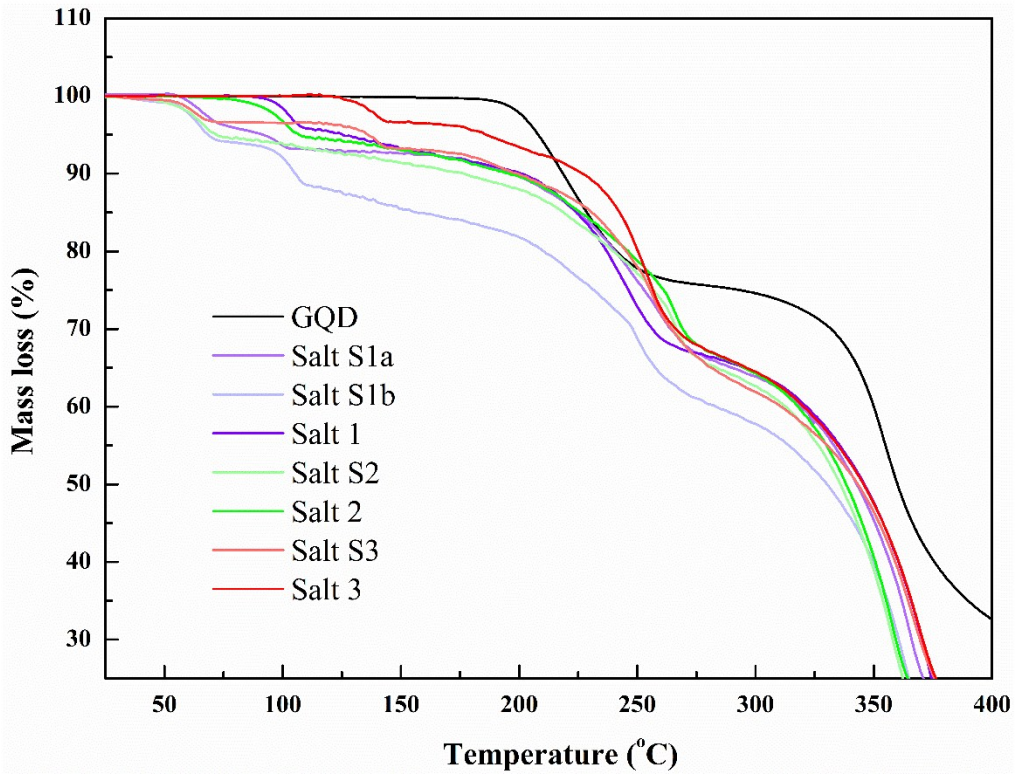

Figure S11. The overlaid TGA profiles of various forms.

Figure S12

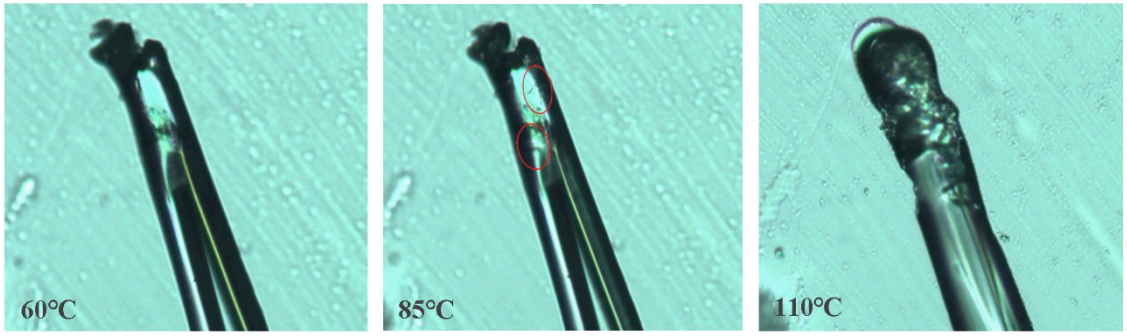

Figure S12. Desolvation process using HSM. Here we take salt S2 as a represented example. The HSM photograph showed that when it desolvated by heating, the color of the birefringence of the crystal changed from 60°C to 85°C and finally melted at about 110°C.

Figure S13

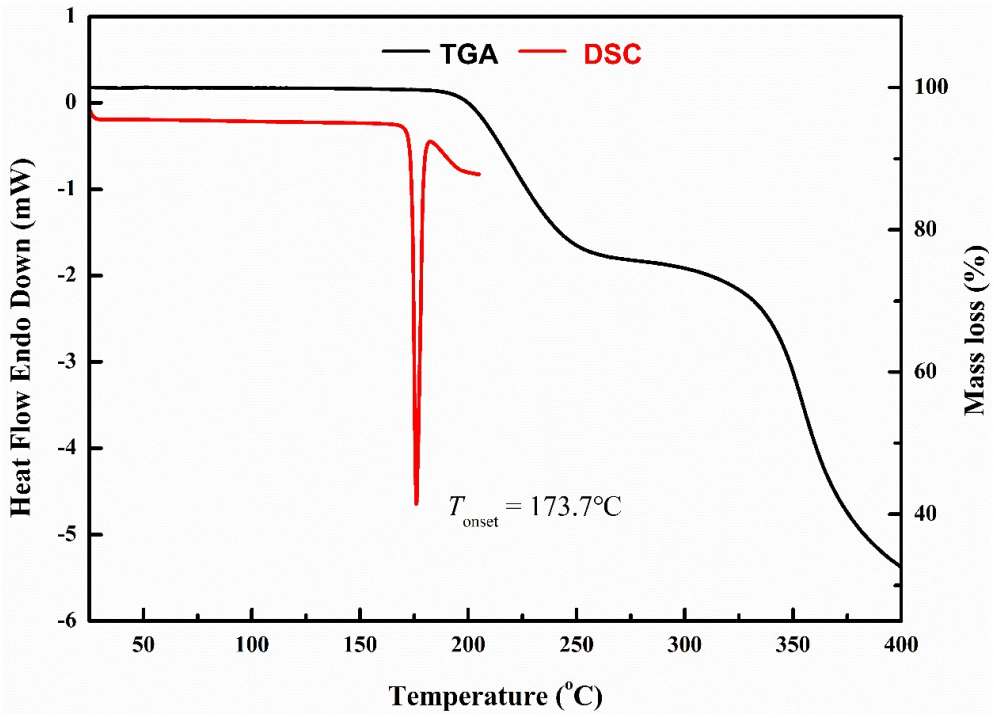

(a)

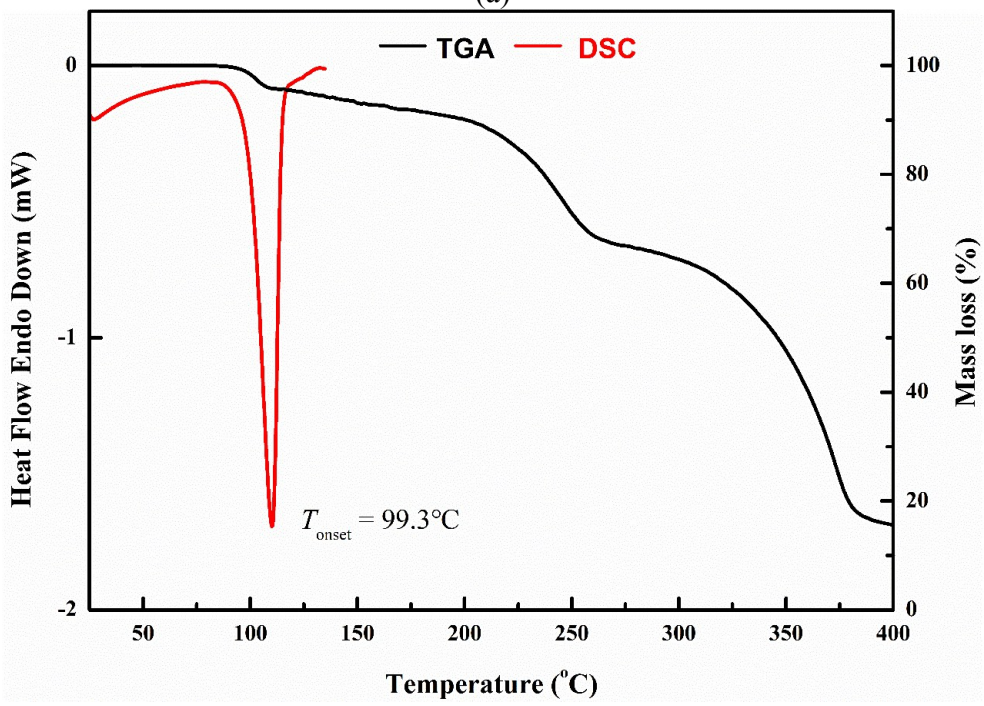

(b)

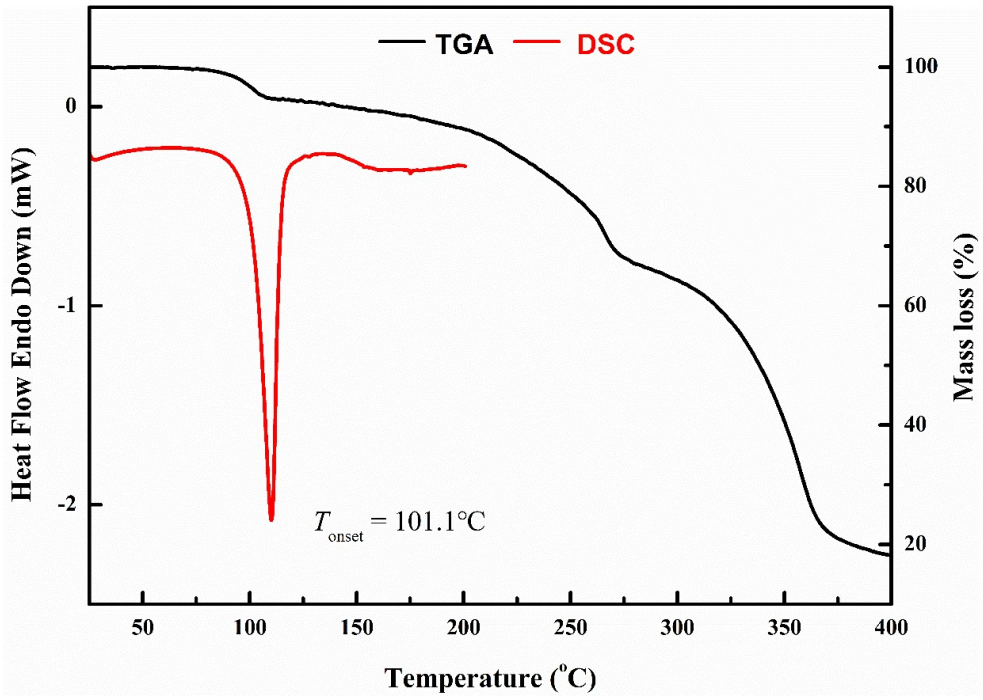

(c)

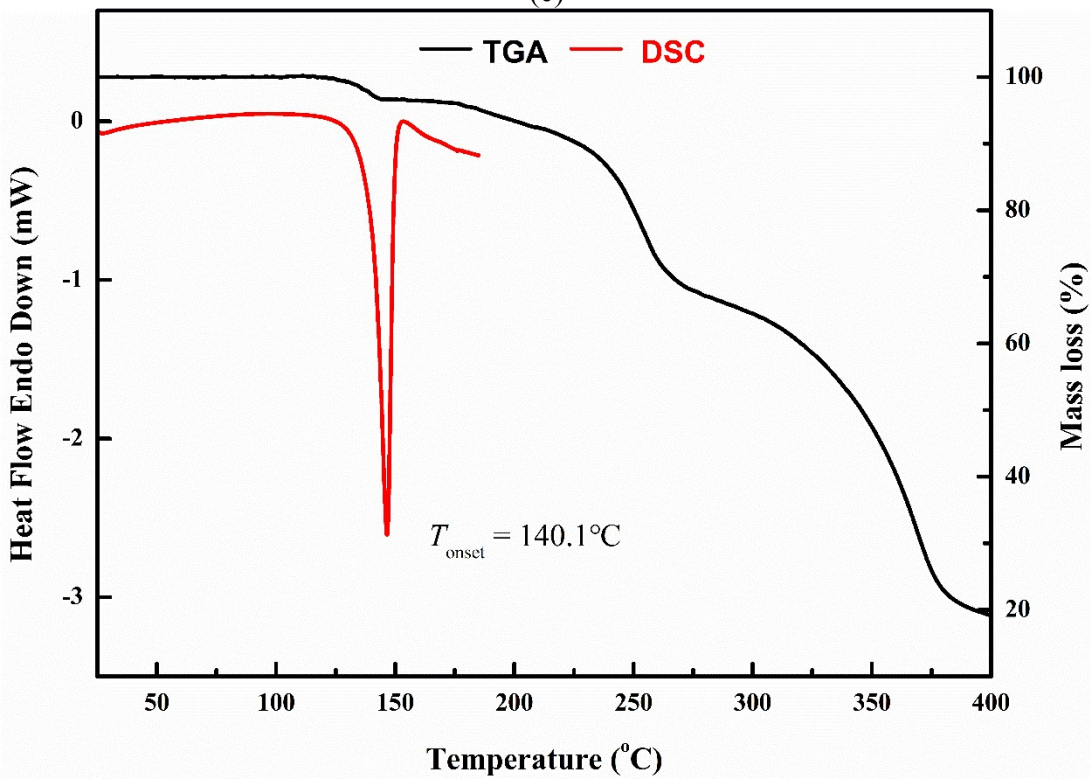

(d)

Figure S13. The overlaid DSC and TGA profiles of (a) GQD, (b) salt 1, (c) salt 2 and (d) salt 3.

Figure S14

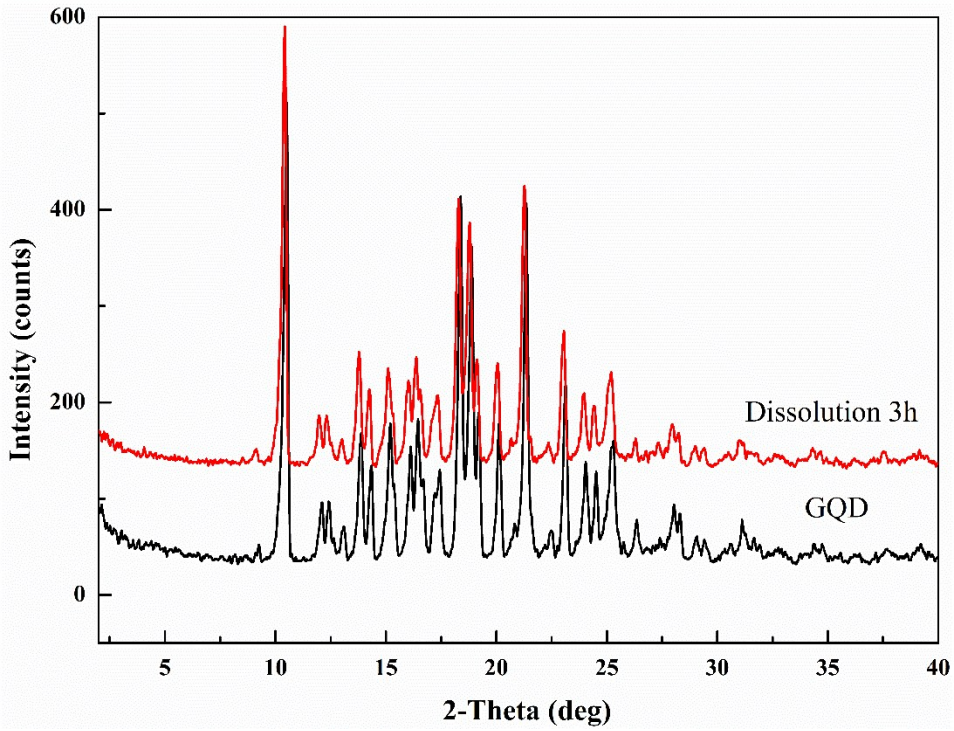

(a)

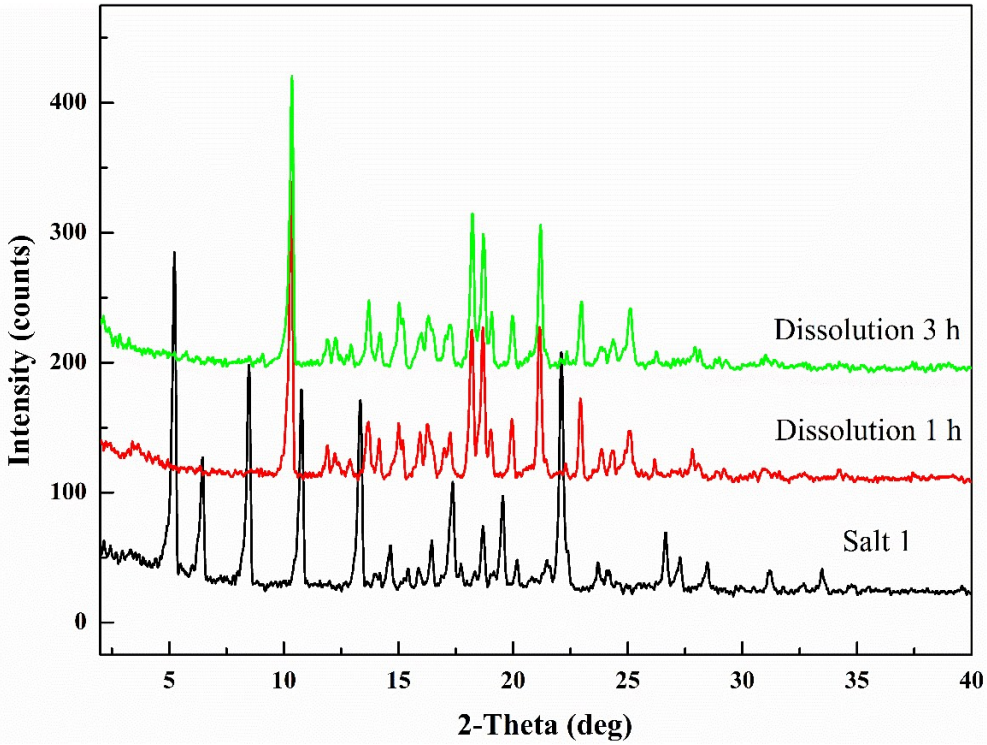

(b)

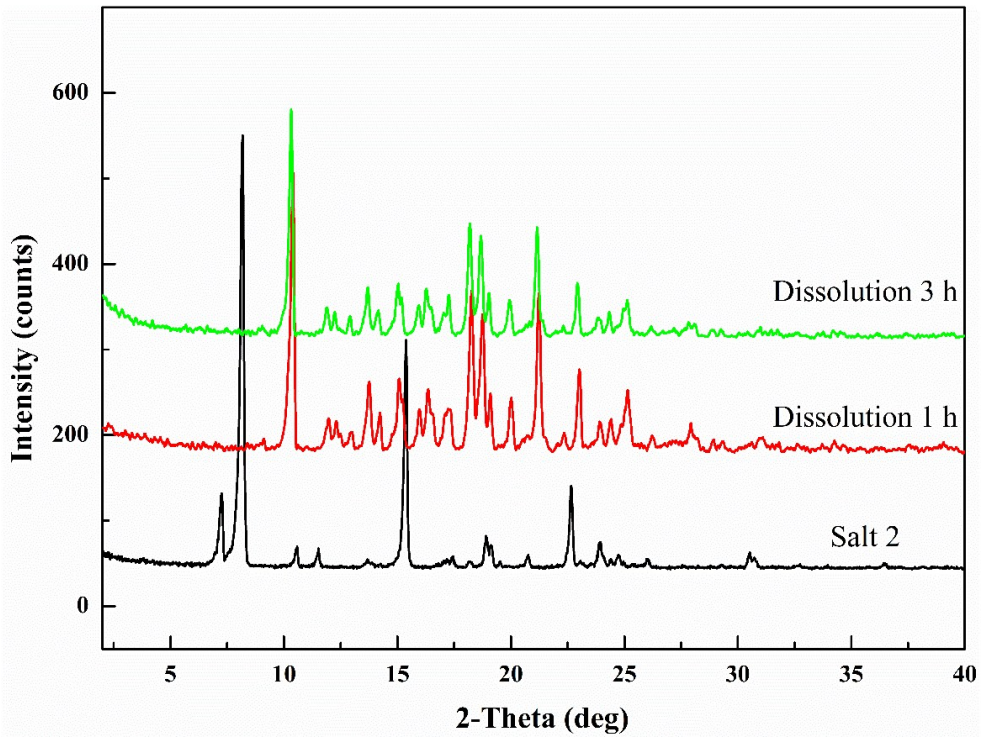

(c)

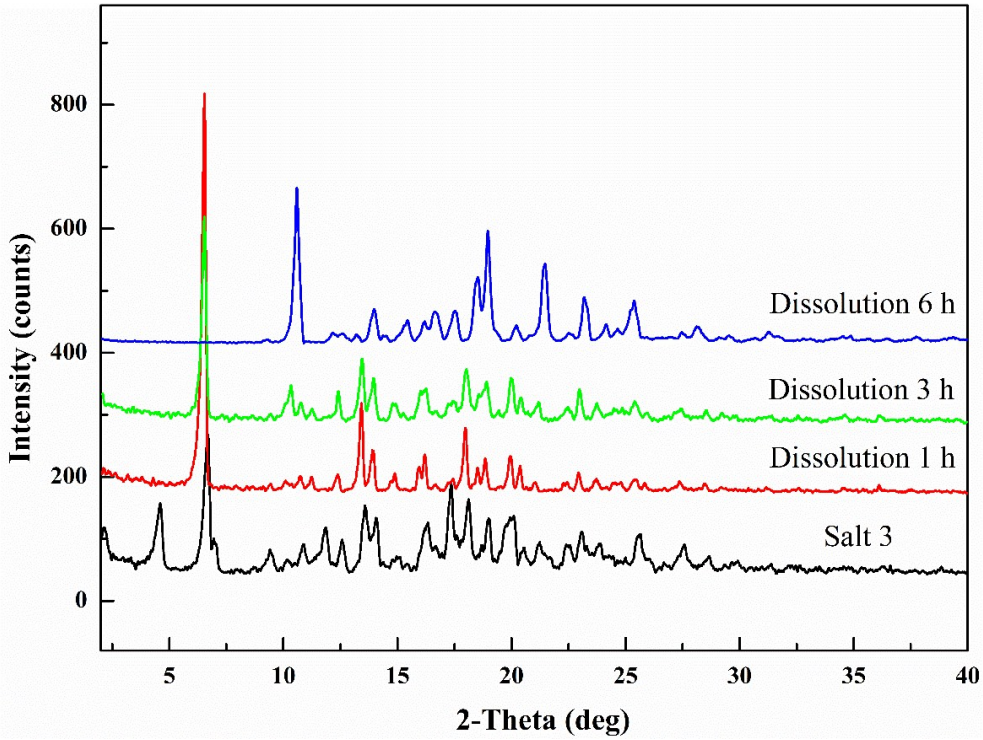

(d)

Figure S14. PXRD pattern of the powder after contact with dissolution media, (a) GQD, (b) salt 1, (c) salt 2 and (d) salt 3.